ENGINEERING RESEARCH INSTITUTE
THE UNIVERSITY OF MICHIGAN
ANN ARBOR

AN EVALUATION OF A SPECIAL BROADBAND RECEIVER INPUT CIRCUIT

Technical Report No. 67
Department of Electrical Engineering
Electronic Defense Group

By: B. F. Barton
D. Hamburg

Approved by: *[signature]*

A. B. Macnee

TABLE OF CONTENTS

LIST OF ILLUSTRATIONS

Page

ABSTRACT

A theoretical discussion of a somewhat novel
broadband receiver input circuit is presented. The
circuit utilizes two crystals, one in a chopper which
acts on the incoming signal, and a second in a subsequent
envelope detector. The amplifier which follows can be
band pass rather than video, as in the conventional
crystal video circuit. Various problems related to
sensitivity are discussed. Considerable experimental
data which corroborates the discussion are also included.

ELECTRONIC DEFENSE GROUP

TECHNICAL REPORT No. 67

ERRATA

Page

1   Should be Task Order EDG-4

10   Comma after "amplifier".

12   Fig. 7 f_i should be f_m.

13   Paranetheses missing at end of line 9.

13   Should be e'_{out} in bottom line instead of e'.

22   Should be minus sign in front of 52.0 dbm for 1N21B(6).

27   Footnote 1 - Should be Fig. 19 (Not Fig. 21).

28   Fig. 18, line 3 -- omit diagonal line after -62.9.

32   Last equation should have 4 in denominator instead of 2.

AN EVALUATION OF A SPECIAL BROADBAND RECEIVER INPUT CIRCUIT

I. INTRODUCTION

The receiver input circuit shown in Fig. 1 was recently developed by

Mr. Herbert Brett at Evans Signal Laboratory.[*] A number of other forms of

this circuit have been investigated at Evans, but it is believed that the

principle of operation is the same in each case. Phenomenologically, it has

been observed that if a modulated RF signal and a sinusoidal external generator

signal are impressed on the circuit as shown, the modulation can be transferred

to a carrier at the external generator frequency independently of the RF carrier

frequency. It is also possible to transfer the modulation to carrier frequencies

which are harmonics of the external generator fundamental frequency.
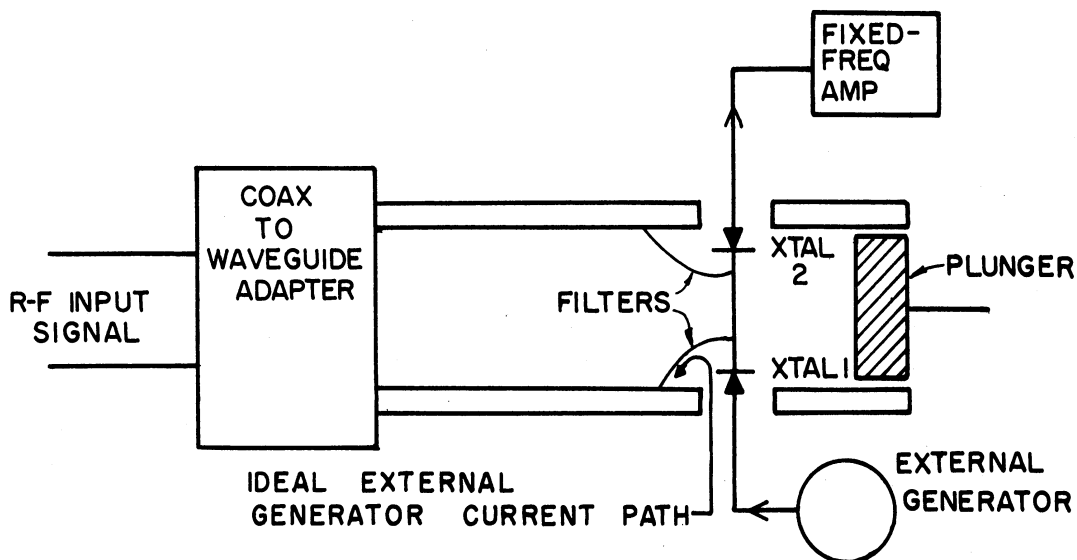
FIG. 1 BRETT RECEIVER INPUT CIRCUIT

[*] The analysis and measurements described in this report were carried out at
the request of Evans Signal Laboratory.

In the Appendix it is demonstrated that the operation of the circuit
of Fig. 1 can be interpreted as in Fig. 2. An input signal of carrier frequency
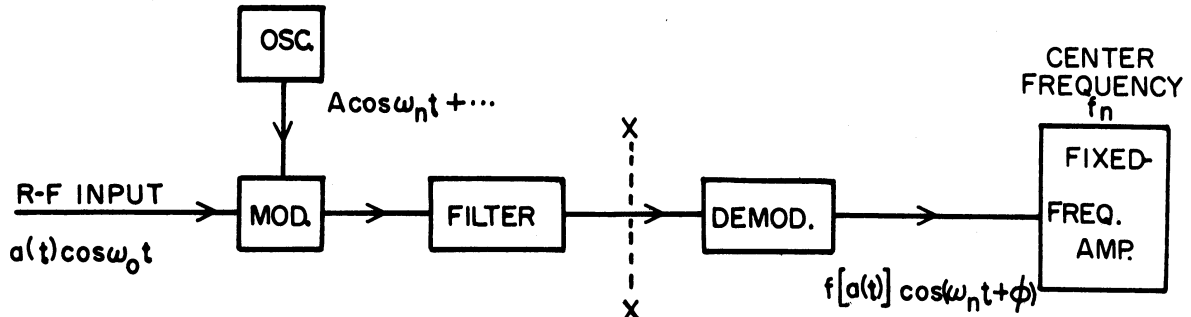
FIG.2 ASSUMED EQUIVALENT CIRCUIT OF FIG.1

f_0 with modulation $a(t)$ is initially modulated. This is accomplished in the

circuit of Fig. 1 by crystal 1. The waveform of the modulation resulting at

crystal 1 may be supposed to have a Fourier Series representation containing

a component (at frequency f_n) of interest. After filtering out undesired

components such as at the oscillator fundamental frequency and harmonics,

demodulation (at crystal 2 in Fig. 1) produces a signal of carrier frequency f_n

with modulation $f\left[a(t)\right]$; i.e., the modulation at the output of the circuit is

a function f of the input modulation. In contrast to a crystal video circuit

where subsequent amplification is video, the subsequent amplification of the

above circuit is centered around a frequency f_n. The circuit is similar to a

crystal video circuit, however, in that envelope detection occurs prior to

amplification. In a superheterodyne receiver, on the other hand, higher

sensitivities are achieved by avoiding such a low level of detection. The

comparison is expressed mathematically in the Appendix.

The application of a circuit such as Fig. 1 in a broadband (microwave)

receiver has been suggested. A loss of somewhat more than 3 db is expected

in a crystal modulator.[1] This advantage, relative to a conventional crystal video receiver, might be substantially offset through the use of a phase-sensitive second detector, provided the circuit between the modulator and demodulator is non-dispersive over the RF band.[2]

2. SUMMARY OF CRYSTAL THEORY

A principle remaining factor necessary for a sensitivity comparison between the circuit of Fig. 1 and the crystal video circuit is detector efficiency. In References 2 and 3 material is presented from which the following conclusions are drawn:

The output signal to noise voltage ratio of a crystal detector is given by

$$\frac{E}{N} = \frac{P}{\sqrt{4kTB}} M \tag{1}$$

where M is called the figure of merit and is given by

$$M = \frac{\beta R}{\sqrt{Rt + R_a}} \tag{2}$$

where,

P = RF power into crystal,

R = video (or output) crystal resistance,

β = current sensitivity = $\dfrac{\text{current out (amps)}}{\text{power in (watts)}}$,

t = effective crystal noise temperature ratio, and

R_a = equivalent noise resistance of the subsequent amplifier.

Note that the figure of merit depends on the noise characteristics of the amplifier following the detector.

---

1. It is assumed that for a fixed character of input signal envelope the detectability is measured by the average signal power absorbed by crystal 2 of Fig. 1.

2. An advantage of 3 db accrues for a phase sensitive detector (Ref. 1) compared to a linear detector at unity output signal to noise ratio, if the noise is noncoherent. Larger advantages can be realized at lower signal to noise ratios.

The output noise from a crystal consists of Johnson noise plus additional components in the presence of excitation. The amplitude of the excitation induced noise varies inversely with frequency over a range of frequencies from at least 50 cps to 60 mc. The parameter t is thus a function of output frequency; i.e., the average value of t over a narrow band around a frequency f is referred to as the value of t at the frequency f. The parameter t varies widely with the degree of excitation. Values as high as 100,000 have been observed with reverse bias in the neighborhood of 50 cps. In the presence of a typical size local oscillator signal, large values of t are observed at audio frequencies. The value of t is typically less than 1.5 in the frequency range above perhaps 30 mc with the usual local oscillator drive, however, which accounts in part for the choice of conventional intermediate frequencies.

In the absence of excitation, the laws of thermodynamics require that the crystal noise temperature (ratio) t be unity. Now, if only a signal to be detected is applied to a crystal, the output noise power available in a limited frequency band is well below the input power. It has, in fact, been established experimentally that if _only_ a signal near the limit of sensitivity is applied, the effective value of t is unity; i.e., the excitation induced noise output does not in this case limit sensitivity.[1] Applying this result in Eqs 1 and 2, it is found that at unity output signal to noise ratio and with only a signal to be detected applied,

$$P = \frac{\sqrt{4kTB}}{M} = \frac{\sqrt{4kTB}}{\beta} \frac{\sqrt{R+R_a}}{R} \tag{3}$$

1. See Ref. 2, pg. 346 and Ref. 3, p. 8. The assumption of unity noise ratio may be invalid below some frequency due to the 1/f character of the excess noise. This point is discussed in Section 3 along with flicker noise of the amplifiers, which has a similar character.

Experimental studies indicate that for a video frequency output band the optimum M occurs at essentially zero bias. This is expected since t has been noted to increase extremely rapidly at low frequencies in the presence of excitation.

It is interesting to consider whether a significant increase in M might be obtained by utilizing a crystal bias at a detector output center frequency above perhaps 10 mc. In this frequency range t $\approx$ 1 even for biases of a substantial fraction of a volt. Further, the ideal crystal characteristic,

$$i = I_o\left(e^{\frac{qV}{kT}} - 1\right), \tag{4}$$

indicates a monotonically increasing curvature (and thus β) with increasing forward bias. An actual crystal characteristic becomes linear for large forward signals, however, so that an experimental curve of β vs forward bias may be expected to be in the form suggested by Fig. 3. If a transformer of turns ratio
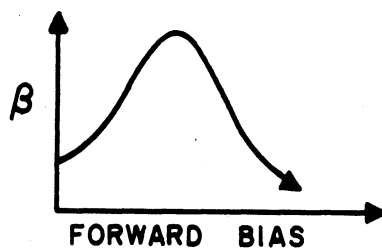

FORWARD BIAS

FIG. 3

1:n at the crystal output and t $\approx$ 1 are assumed, then

$$M = \frac{\beta nR}{\sqrt{n^2R + R_a}} \tag{5}$$

If, favorably, one makes

$$n^2R \gg R_a \; ,$$

then

$$M \simeq \beta \sqrt{R} \; .$$

Elementary theory indicates that M should increase with forward bias under these conditions. Specifically:

$$\Delta i = I_0 \left(e^{\frac{qV_b}{kT}} e^{\frac{q\Delta V}{kT}} - 1 \right) - I_0 \left(e^{\frac{qV_b}{kT}} - 1 \right) = I_0 \, e^{\frac{qV_b}{kT}} \left(e^{\frac{q\Delta V}{kT}} - 1 \right) \tag{6}$$

From Eq 6, for small ΔV,

$$\frac{\Delta V}{\Delta i} = R = \frac{kT}{qI_0} \, e^{-\frac{qV_b}{kT}} . \tag{7}$$

Since

$$\beta = K \frac{\partial i}{\partial V_b} = K \frac{qI_0}{kT} \, e^{\frac{qV_b}{kT}} , \tag{8}$$

then,

$$M \approx K \sqrt{\frac{qI_0}{kT}} \, e^{\frac{qV_b}{2kT}} . \tag{9}$$

For actual crystals, both β and R decrease rather rapidly beyond a certain small bias. It therefore seemed worthwhile to determine experimentally whether an increase in sensitivity occurs with moderate bias as the detector output center frequency is raised above perhaps 10 mc.

3. SOME ELEMENTARY NOISE CONSIDERATIONS

Before describing the experimental evaluation of the Brett circuit (Fig. 1), it is worthwhile to discuss briefly some noise problems which are of importance in assessing the advantages of a receiver employing this circuit compared to a video or superheterodyne system. These problems have to do with flicker noise, the 1/f crystal noise spectrum already mentioned, and the design of the input circuit of the amplifier following the detector crystal.

Flicker noise[1] in tubes is thought to occur as a result of a "shimmering" of the emission from the cathode surface. Flicker noise results in an equivalent

---

1. Extensive measurements of flicker noise characteristics have been made at the University of Minnesota under Professor August Van der Ziel.

tube noise resistance plot with frequency similar in shape to that of Fig. 4.[1]

The ordinate is proportional to available tube output noise power. The noise

depicted consists in part of shot noise which is essentially independent of

frequency and is the principal noise contribution at the high frequency end

of the graph. The other major noise contributions is flicker noise which has

nearly a 1/f power spectrum.

In a broadband microwave monitoring application, input modulation

bandwidths of the order of 1 mc would be likely. It is apparent that even

large excess (flicker) noise components over a band of a few kilocycles per

second may only moderately increase the rms value of the output noise of a

receiver with a 1 mc bandwidth. Further, this audio frequency noise would

be relatively ineffective in masking, for example, 1 μ sec pulses. The

sensitivity for a given signal should depend rather critically on the signal

to noise ratio existing in a limited frequency region containing the first

few harmonics of the input modulation. As the center frequency of this limited

frequency region is lowered, one would expect that the sensitivity would remain

nearly constant until flicker noise became substantial in the region. The

sensitivity should then decrease at roughly 3 db per octave, with further

decreases in center frequency.

The above facts suggested the use of a narrow band filter, centered

around the input modulation fundamental frequency component, for measuring

sensitivity in the experimental circuit. A substantial advantage of this

technique is that relative sensitivities can be determined from meter readings,

by observing the RF signal level at which a high prescribed narrow band signal-

to-noise ratio is realized. For the tests described in Section 5 a three to

---

1. The 6CB6 is one of the best tubes commercially available for applications
   where low flicker noise is desired. Other good tubes in this respect are
   the WE416A, Phillips EF40, and the 6AG5. It is in general advisable to
   select tubes.
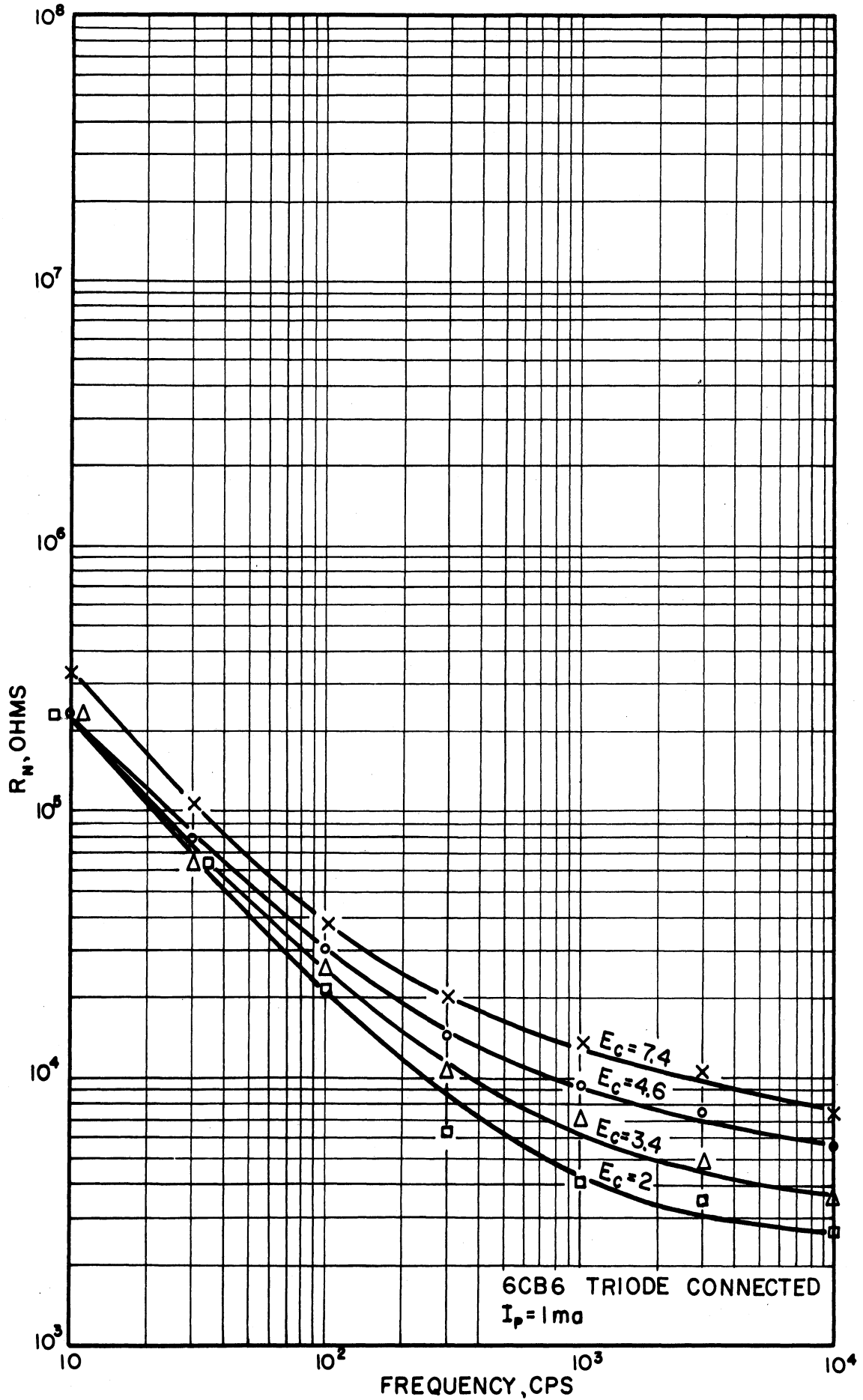
FIG. 4. EQUIVALENT TUBE NOISE RESISTANCE (After Van der Ziel)

one "signal-plus-noise" to "noise" criterion for an 8 cps band centered at

about 1.1 kc was used. The input signal modulation was a 1.1 kc sinusoid.

The 3:1 S+N/N ratio is estimated to correspond to a somewhat less than unity

signal-to-noise ratio for a video system with a bandwidth from 10 cps to

250 kc. The objective of the experimental study was to make a comparison

between the sensitivities of a system employing the Brett circuit and a crystal

video system, rather than to measure the absolute sensitivities achievable.

The meter criterion permitted this comparison to be made easily.

The expected noise variation with frequency at the output of the

second detector is in the form of Fig. 5. A pulse envelope spectrum and a

narrow band filter characteristic are also illustrated. The noise amplitude
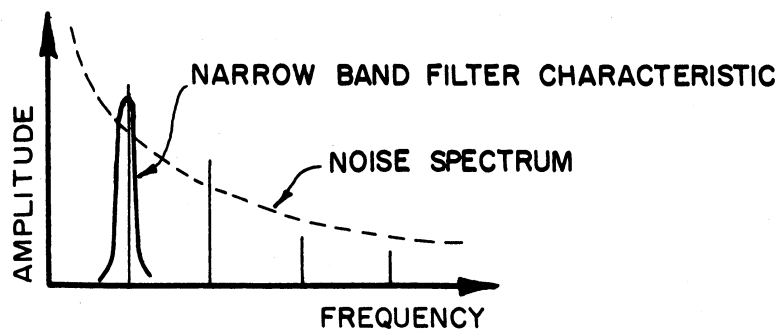
FIG. 5 ILLUSTRATION OF OUTPUT SPECTRA

is a function of frequency, as previously described, so that the "sensitivity"

using the above meter criterion can be expected to vary at low input modulation

frequencies. The sensitivity decreases with decreasing frequency when flicker

or 1/f noise becomes appreciable compared to tube shot noise or Johnson noise.

At this frequency the spot noise figure starts to disintegrate.

The output impedance of the low level detector crystal depends on the

crystal type and sample and crystal bias. A source impedance exists, for a

given fixed frequency amplifier which produces the minimum obtainable noise figure. An analysis of this problem is presented in Ref. 4 . It is shown that the optimum noise factor,

$$F_{opt} = 1 + 2 \frac{R_{eq}}{R_{s\ opt}} \qquad (10)$$

where R_{eq} is the equivalent noise resistance for the input tube and its load. R_{sopt} is the optimum source impedance given by

$$R_{sopt} = \sqrt{\frac{R_g R_{eq}}{T_g/T}} \qquad (11)$$

where R_g = input resistance of the tube and input circuit

$\frac{T_g}{T}$ = input resistance temperature to ambient temperature ratio

For other source impedances

$$F = 1 + \frac{T_g}{T} \frac{R_s}{R_g} + \frac{R_{eq}}{R_s} \left(1 + \frac{R_s}{R_g}\right)^2 \qquad (12)$$

For the cascode input circuits utilized, R_{eq} is known to sufficient accuracy. R_g and R_s are determined using the circuit of Fig. 6. The frequency of the

FIG. 6

high impedance source is varied with R_s removed and, if the amplifier is sufficiently broadband, R_g is determined from the 3 db bandwidth of the response. A similar measurement with the source connected determines R_s. The noise factor of the fixed frequency amplifier was estimated from the data obtained using this
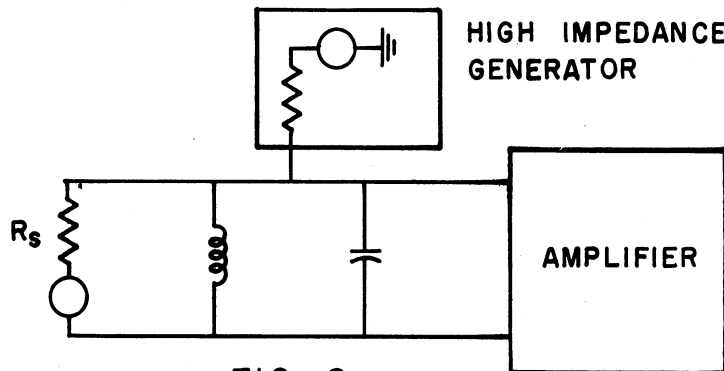
procedure. The sensitivity data were corrected to .5 db noise figure at 2 mc and 2. db at 60 mc.[1]

It is noted that the bandwidth varies with the source impedance in the above circuit. The amplifier is followed in the experimental circuit by a linear detector. Further, the zero signal noise output of the linear detector is sampled at a frequency much lower than the bandwidth of the amplifier. This noise is relatively independent of the bandwidth of a fixed gain amplifier under these conditions (see Ref. 5). It is concluded that the noise factor correction previously described is sufficient for the relatively high signal-plus-noise to noise ratio utilized at the linear detector output.

4. DESCRIPTION OF EXPERIMENTAL TECHNIQUES UTILIZED IN THE INVESTIGATION

Two experimental methods were employed in obtaining the data in this report. Some sensitivity measurements were made directly on the circuit of Fig. 1. The second method of measurement stems from the explanation of the circuit operation which was illustrated in Fig. 2. It is easily shown than the spectrum of a filtered, twice sinusoidally amplitude modulated signal (as assumed at x-x in Fig. 2 in the Introduction), has the form of Fig. 7. If either or both modulations are not sinsuoidal, additional sidebands are present. Then the demodulation process can be regarded as mixing of the carrier and external generator frequency sidebands. The significant difference between this circuit and the conventional superheterodyne circuit is that the two signals in Fig. 7 are of comparable size, while in the superheterodyne mixer one of the signals (the local oscillator signal) is much larger. From this viewpoint, one sees

1. An alternative was to actually optimize the input match for each run.

f_o = SIGNAL CARRIER FREQUENCY
f_1 = SIGNAL MODULATION FREQUENCY
f_n = EXTERNAL GENERATOR FREQUENCY
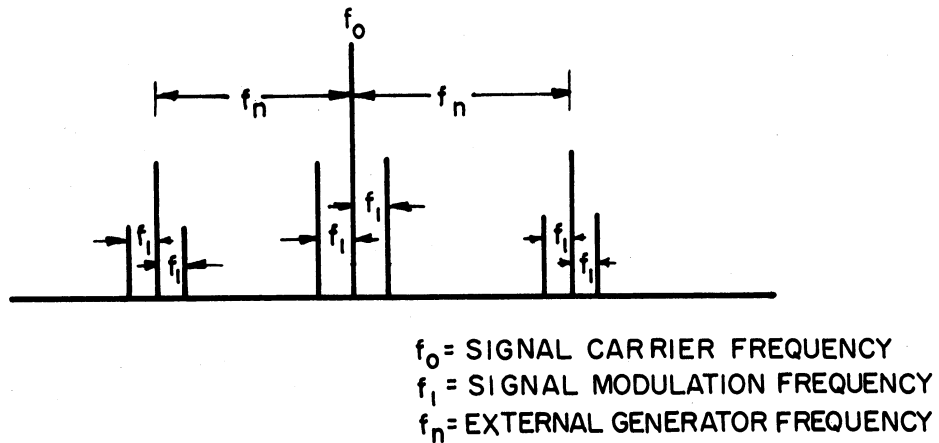
FIG. 7. TWICE AMPLITUDE MODULATED SIGNAL
SPECTRUM

that the desired modulator output centered at f_n will be obtained with the

input of Fig. 8 where one of the groups of sideband spectra has been omitted.

Since the signals are small, the reduction of sensitivity caused by this

omission can be calculated assuming a square-law demodulator characteristic.
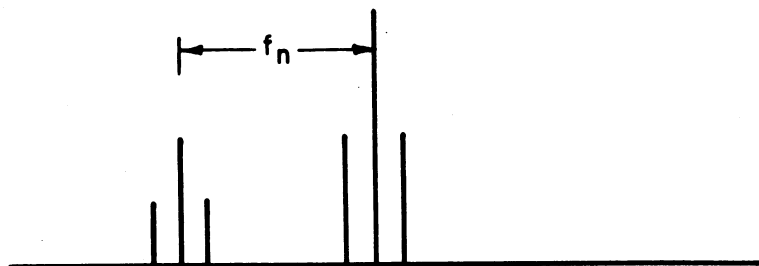
FIG. 8. SYNTHESIZED DEMODULATION CRYSTAL INPUT

Sensitivity comparisons can thus be made using a carrier and a sideband signal

whose frequency separation is the desired external generator frequency, both

signals being modulated by some prescribed (input) modulation signal. The

advantage of synthesizing the modulator output rather than using the actual

circuit is that tests at various RF center frequencies and external generator

frequencies can be made without having to construct a series of modulators

and filters. The advantage of omitting one sideband is that the problem of phasing three oscillators representing the carrier and both sidebands is avoided.

Let the twice modulated signal at x-x in Fig. 2 be

$$e = E(1 + m_m \cos \omega_m t)(1 + m_n \cos \omega_n t) \cos \omega_0 t$$

$$= E(1 + m_m \cos \omega_m t) \cos \omega_0 t + \frac{E}{2} m_n (1 + m_m \cos \omega_m t) \cos (\omega_0 - \omega_n)t \qquad (13)$$

$$+ \frac{E}{2} m_n (1 + m_m \cos \omega_m t) \cos (\omega_0 + \omega_n)t$$

which corresponds to the spectrum of Fig. 7. When passed through a square law device, and when $m_m = m_n = 1$, the output is

$$(14)$$

$$i_0 = \beta E^2(1 + 2 \cos \omega_m t + 1/2 + 1/2 \cos 2\omega_m t)(1 + 2 \cos \omega_n t + 1/2 + 1/2 \cos 2\omega_n t$$

$$x \ (1/2 + 1/2 \cos 2\omega_0 t)$$

After amplifying at a center frequency ω_n and passing through a linear detector, the output with frequency ω_m is

$$e_{out} = 2\beta \ AE^2 \cos \omega_m t \qquad (15)$$

where A is a gain factor. If, however, one sideband of the RF signal is omitted or filtered, the signal applied to the square law device is in the form

$$e' = E(1 + m_m \cos \omega_m t) \left[\cos \omega_0 t + 1/2 \ m_n \cos (\omega_0 - \omega_n)t \right] \qquad (16)$$

For $m_m = m_n = 1$, the output from the square law device is

$$i'_0 = \beta E^2 (1 + 2 \cos \omega_m t + 1/2 + 1/2 \cos 2 \omega_m t)x$$

$$(17)$$

$$\left[1/2 + 1/2 \cos 2\omega_0 t + 1/2 \cos \omega_n t + 1/2 \cos (2\omega_0 - \omega_n)t + 1/8 + 1/8 \cos 2(\omega_0 - \omega_n)t \right]$$

After amplifying at a center frequency ω_n, and passing through a linear detector, the component with frequency ω_m is

$$e' = \beta AE^2 \cos \omega_m t \qquad (18)$$

13

Hence the omission of a sideband reduces sensitivity of the demodulator

portion of the circuit by 6 db. The experimental circuit based on this

analysis will be referred to as the synthesized Brett system.

5. SYNTHESIZED SYSTEM MEASUREMENTS

In making sensitivity measurements with the synthesized Brett system,

the parameters varied were RF frequency, chopper[1] frequency, demodulator

crystal (type and sample), and crystal bias. The sensitivity data thus obtained

were compared with crystal video data obtained at the same RF frequencies

after converting the experimental setup to a video system.

5.1 Basic Setup

A block diagram of the basic experimental setup for the synthesized

system investigation is shown in Fig. 9. As pointed out earlier, the input

to the demodulator crystal (crystal 2 in Fig. 1) of the Brett circuit can be

effectively synthesized with two commonly-modulated signals whose difference

frequency is the desired chopper frequency. Generators A and B supply the

two RF signals and the audio oscillator (Hewlett-Packard model 200AB) supplies

the common modulation. The 10 db pads in each generator line provide isolation

of the generators while the 10 db pad in the common line makes the impedance

more nearly 50 ohms. The two tuning stubs provide a means of matching the

crystal to the 50 ohm source.[2] The signal out of the demodulator crystal is

amplified by a fixed-frequency amplifier. The particular amplifiers used have

tuned circuit inputs with provision for applying crystal bias.

1. The external generator signal will be referred to as the chopper signal
    in the remainder of the report.
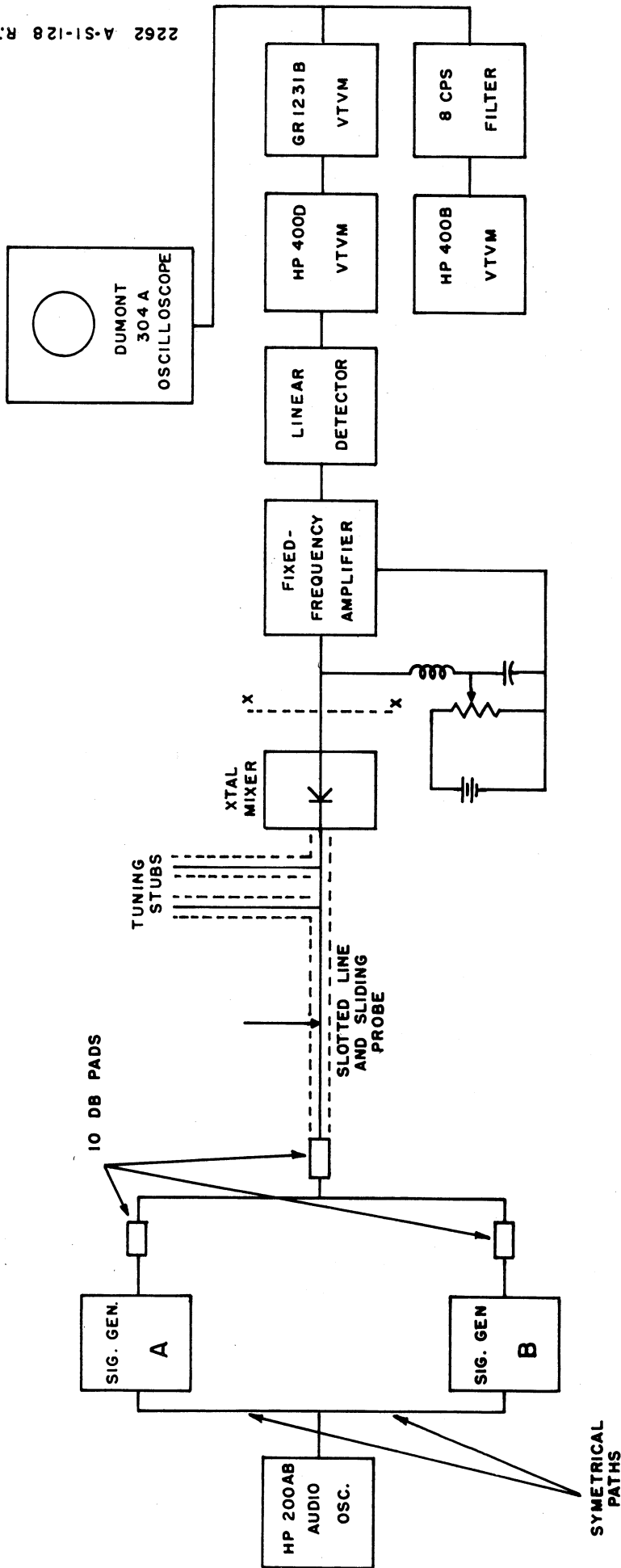2. The RF matching problem is discussed in Section 5.2 .

FIGURE 9

BLOCK DIAGRAM OF EXPERIMENTAL

SETUP USED FOR SYNTHESIZED SYSTEM INVESTIGATION

After sufficient fixed-frequency amplification, a crystal diode detector is used to give linear detection. Subsequent video amplification is provided by the vacuum tube voltmeters (Hewlett-Packard 400-D and General Radio 1231-B). The use of the 8 cps bandwidth filter and the meter criterion was discussed in Section 3 . The 400-B VTVM placed after the filter measures the signal-plus-noise or noise voltages, as the case may be, in the narrow band. It was necessary to incorporate 5000 $\mu\mu f$ in the meter to perform the averaging of the 8 cps band of noise, and a time constant of several seconds resulted. The oscilloscope (Dumont 304-A) provides visual monitoring.

To convert the above setup to a crystal video system, one of the RF generators is turned off, and the fixed-frequency amplifier and the linear detector are removed.

5.2 Basic Procedure

The first step in obtaining a particular sensitivity measurement is to tune generators A and B. One of the generators is tuned to the RF frequency desired and the other to a frequency that causes the difference frequency to fall in the passband of the fixed-frequency amplifier. The second step is to adjust the audio oscillator to the center frequency of the 8 cps bandwidth filter. The third step is to adjust the two tuning stubs to give a maximum signal output as indicated by the HP 400-B VTVM. The fourth step is to adjust the relative attenuator settings of generators A and B until the signal-plus-noise output in the 8 cps video band is three times the noise alone in the same band; i.e., until the meter criterion described is satisfied. Since it is unlikely that an impedance match can be obtained at two different frequencies by means of double-stub matching, the final step is to measure the standing-waves associated with each generators mismatch. Two methods of measurement were employed, depending upon the RF frequency.

For RF frequencies of 200 and 400 mc, the measurement of standing waves was accomplished with a HP 803-A VHF bridge. A block diagram of the setup is shown in Fig. 10. Generators A and B and the 10 db pads are
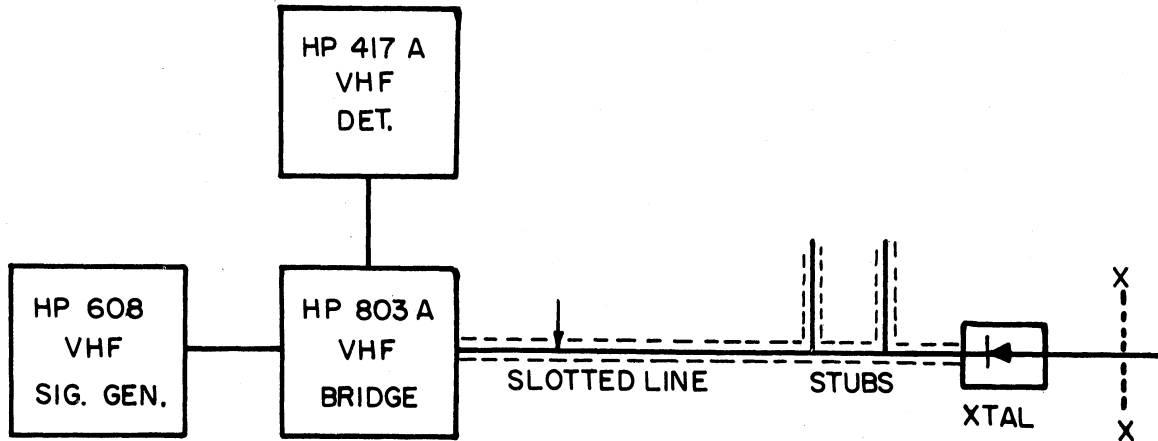
FIG. 10. SETUP FOR MEASURING STANDING-WAVES AT 200 & 400 MC

removed from the setup of Fig. 9 and the VHF bridge with its associated equipment is inserted in their place. The uncorrected impedance at the one generator's frequency is then determined. This impedance is used to obtain the standing-wave ratio in the line of that generator. From the standing-wave ratio, the associated power loss due to mismatch is determined. The measurement is then repeated at the frequency of the other generator, and its power loss due to mismatch is determined.

For the RF frequencies of 1830 and 1950 mc, the measurement of standing-waves was accomplished with a slotted line and sliding probe. Since the RF signal level in the line was quite low, and since a small amount of coupling between the probe and the line was desired, superheterodyne receiver sensitivity was required to detect the signal picked up by the probe as it was moved along the line. A block diagram of the setup is shown in Fig. 11.
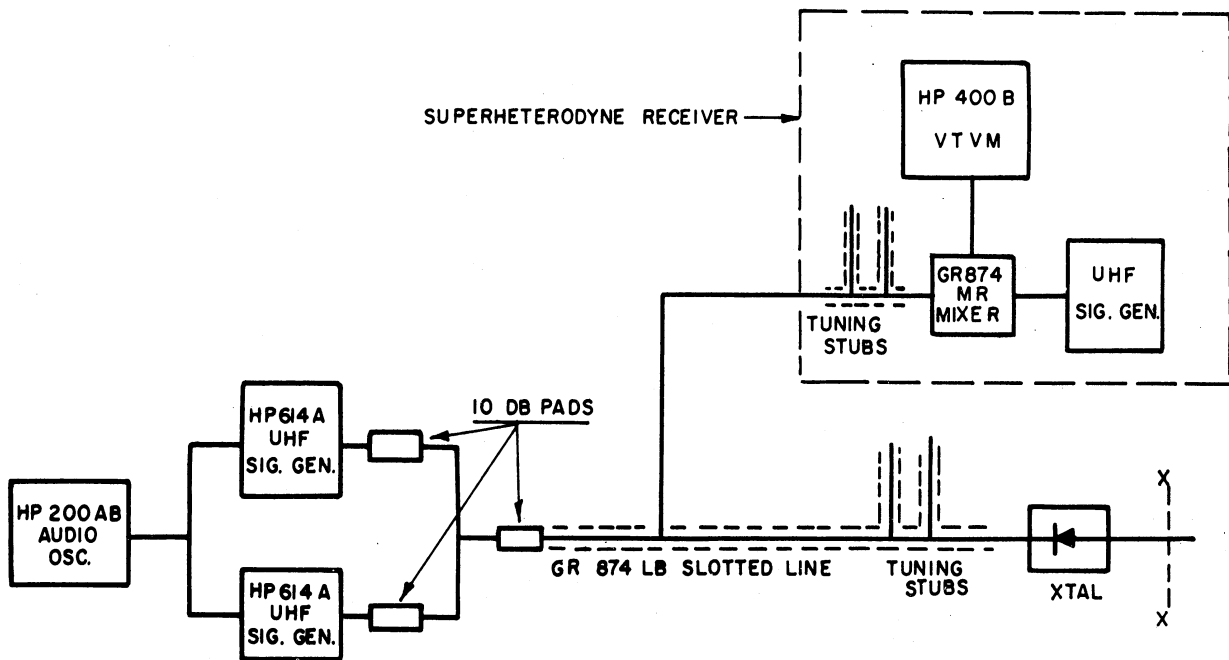
FIG. II. SETUP FOR MEASURING STANDING-WAVES AT 1830 AND 1950 MC

The superheterodyne receiver consists of the two tuning stubs for matching, a

UHF signal generator for heterodyning, a mixer, and a HP 400-B VTVM for

amplifying and indicating the mixer output signal. One of the RF generators

is turned off. The standing-waves measured are then due to the other generator's

mismatch. After the local oscillator frequency and the two stubs in the

superheterodyne receiver circuit are adjusted, the probe is moved along the

slotted line and the maximum and minimum readings on the HP 400-B are recorded.

The voltage-standing-wave ratio is then calculated as follows:

$$\text{VSWR} = \frac{(S+N)^2_{max} - (N_o)^2}{(S+N)^2_{min} - (N_o)^2} \tag{19}$$

where $(S+N)_{max}$ and $(S+N)_{min}$ refer to the maximum and minimum HP 400-B readings

obtained with the generator on, and (N_o) refers to the no-signal noise reading.

From the voltage standing-wave ratio, the mismatch loss for one generator is

determined. The entire procedure is then repeated to obtain the mismatch loss for the other generator.

It was desirable to obtain a number for each run, determined by the RF signal generators' attenuation readings and various corrections that are summarized in Section 5.3, indicative of the sensitivity achieved in the run. This number is referred to in this report as the relative sensitivity. The attenuator reading for the larger of the two RF signals representing the carrier and one sideband of the twice-modulated signal was arbitrarily chosen as the uncorrected reference level. The level of the two signals differed by 6 db, which is the difference between the carrier and sideband of a 100% sinusoidally modulated signal. It was observed that if one attenuator were set higher by a certain amount and the other set lower by the same amount for a particular setup, the output remained unchanged.[1] Therefore, after corrections were applied to the attenuator readings for a particular run, the corrected readings were referred to this 6 db separation.

The above steps were carried out for zero crystal bias on each crystal and the raw data were recorded. The crystal bias was then increased to the point where the signal-plus-noise indicated by the HP 400-B VTVM was maximum, and the bias voltage and sensitivity at this point were recorded. Increasing the crystal bias produced two noticeable effects. The first effect was that the no-signal noise reading decreased steadily and finally reached a constant value. The second effect was that the signal-plus-noise reading initially increased and then dropped off rapidly. It would be expected, then, that the optimum bias would be greater than the bias associated with the maximum HP 400-B VTVM signal-plus-noise reading since the no-signal noise is

---

1. This statement was true as long as the two signals were within perhaps 20 db of each other.

still decreasing at the maximum point. Actually, however, the signal-plus-noise drop-off is so rapid that there is essentially no difference between the true optimum bias and the bias associated with the maximum reading. The bias voltage recorded has thus been referred to as the optimum bias.

The RF frequencies investigated were 200, 400, 1830, and 1950 mc. At 200 and 400 mc, HP 608 VHF signal generators were used for generators A and B. At 1830 and 1950 mc, HP 614-A and HP 616-A UHF signal generators were used.

Chopper frequencies investigated were 60 mc and 2 mc. Both the 60 mc and the 2 mc fixed frequency amplifiers have a cascode input circuit. The noise figure of the 60 mc amplifier measured with a 4,000 ohm generator was about 3 db. The noise figure of the 2 mc fixed-frequency amplifier measured with a 12,000 ohm generator was also about 3 db.

The corresponding crystal video sensitivities are obtained as above, except there is only one RF generator to tune and no difference frequency adjustments to be made. Furthermore, the measurements are made only at zero crystal bias since it was determined experimentally that this was essentially optimum.

5.3 Results of Synthesized System Measurements

The raw data for the synthesized Brett system and the corresponding crystal video system are presented in Fig. 12. The sensitivities in Fig. 13 are relative sensitivities; i.e., the various corrections previously discussed have been applied. These corrections are associated with RF mismatch loss (discussed in Section 5.2), omission of the one side band in the synthesized signal (discussed in Section 4), fixed-frequency amplifier input circuit noise figure variation with crystal type and bias (discussed in Section 3), different peak voltages between the synthesized signal and the crystal

Crystal Type	Freq. (mc.)	Crystal Video Sensitivity (dbm)	60 mc Difference Frequency Sensitivity (dbm)		2 mc Difference Frequency Sensitivity (dbm)	
			O bias	Opt. bias	O bias	Opt. bias
1N56 [1]	200	-49.5				
1N56	400	-48.0				
1N82A [2]	200	-55.0	-36.5	Opt bias is 0	-50.2	-51.5 (.04 v.)
1N82A	400	-58.0	-39.5	Opt bias is 0	-48.0	-50.0 (.035 v.)
1N82A [3]	200	-50.5				
1N82A	400	-54.5				
1N69 [4]	200	-52.0	-35.0	Opt bias is 0	-44.5	Opt bias is 0
1N69	400	-49.0	-35.0	Opt bias is 0	-40.0	Opt bias is 0
1N21B [6]	200	-46.0	-29.5	-39.5 (.14 v.)	-42.5	-43.0 (.12 v.)
1N21B	400	-49.5	-33.0	-42.2 (.134v.)	-42.0	-47.0 (.11 v.)
1N21B	1830		-33.5	-42.5 (.13 v.)		
1N21B	1950		-33.0	-42.5 (.15 v.)		
1N21B [11]	1830	-56.4	-38.5	-44.5 (.08 v.)	-45.5	Opt bias is 0
1N21B	1950	-59.1	-38.7	-43.0 (.065 v.)	-47.5	-48.0 (.02 v.)
1N21B [12]	1830	-54.0	-34.5	-44.0 (.10 v.)		
1N21B	1950	-55.5	-33.7	-41.0 (.17 v.)		
1N21A [13]	1830	-54.0	-34.0	-41.0 (.17 v.)		
1N21A	1950	-55.5	-33.7	-41.0 (.17 v.)		
1N23 [14]	1830	-52.3	-35.5	-44.0 (.09 v.)	-42.5	-46.5 (.05 v.)
1N23	1950	-54.2	-35.5	-42.0 (.09 v.)	-45.0	Opt bias is 0
1N23 [15]	1830		-36.0	-43.5 (.10 v.)		
1N23	1950		-36.5	-43.0 (.09 v.)		

UNCORRECTED SENSITIVITIES OBTAINED WITH

SYNTHESIZED BRETT SYSTEM

Figure 12

NOTE:
Superscripts on crystal types designate particular samples.

Crystal Type	Freq. (mc)	Crystal Video Sensitivity (dbm)	60 mc Difference Frequency Sensitivity (dbm)		2 mc Difference Frequency Sensitivity (dbm)	
			0 bias	Opt. bias	0 bias	Opt. bias
1N82A[2]	200	-61.6	-49.3	Opt. bias is 0	-53.1	-53.4 (.04 v.)
1N82A	400	-63.6	-49.7	Opt. bias is 0	-52.6	-52.7 (.04 v.)
1N69 [4]	200	-55.0	-48.2	Opt. bias is 0	-48.2	Opt. bias is 0
1N69	400	-50.5	-45.0	Opt. bias is 0	-43.1	Opt. bias is 0
1N21B[6]	200	52.0	-44.2	-46.4 (.14 v.)	-45.5	-49.8 (.12 v.)
1N21B	400	-51.8	-43.1	-44.6 (.13 v.)	-44.9	-48.7 (.11 v.)
1N21B[11]	1830	-56.4	-52.0	Cpt. bias is 0	-49.8	Opt. bias is 0
1N21B	1950	-59.1	-52.7	Opt. bias is 0	-52.6	Opt. bias is 0
1N23 [14]	1830	-52.3	-49.2	-49.8 (.09 v.)	-47.0	-49.8 (.05 v.)
1N23	1950	-54.2	-48.2	-49.9 (.09 v.)	-49.6	Opt. bias is 0

Figure 13

CORRECTED SENSITIVITIES OBTAINED WITH

SYNTHESIZED BRETT SYSTEM

NOTE:
Superscripts on crystal types designate particular samples.

video input signal[1], and different signal generator calibrations.[2]

The above mentioned sensitivities were obtained using an input modulation frequency of about 1.1 kc. For one particular setup[3] the input modulation frequency was varied from about 275 to 4600 cps. There was essentially no change in the synthesized Brett system sensitivities as expected, while the crystal video sensitivities varied as shown in Fig. 14.

6. BRETT CIRCUIT MEASUREMENTS

In making sensitivity measurements with the actual Brett circuit (sketched in Fig. 1), the parameters varied were RF frequency, chopper frequency, and chopper voltage. The sensitivity data thus obtained was compared with crystal video data obtained at the same RF frequencies after converting the experimental setup to a crystal video setup.

6.1 Setup

A block diagram of the setup for obtaining sensitivity data with the Brett circuit is shown in Fig. 15. The HP 620-A SHF signal generator supplies

---

1. The synthesized double modulated signal can be written

$$e_1 = E_1(1 + m_m \cos \omega_m t)(1 + m_n \cos \omega_n t) \cos \omega_0 t.$$

For m_m and $m_n = 1$, the peak value of this signal is $4E_1$.
The crystal video input signal can be written

$$e_2 = E_2(1 + m_m \cos \omega_m t) \cos \omega_0 t.$$

For $m_m = 1$, the peak value of this signal is $2E_2$.
Thus, to correct to the same peak input voltage, the synthesized signal for which the carrier level is taken as reference must be penalized 6 db.

2. One generator was calibrated in terms of the other by first using one and then the other in a crystal video setup.

3. 1N82A crystal No. 2, RF frequency of 400 mc, and chopper frequency of 2 mc.
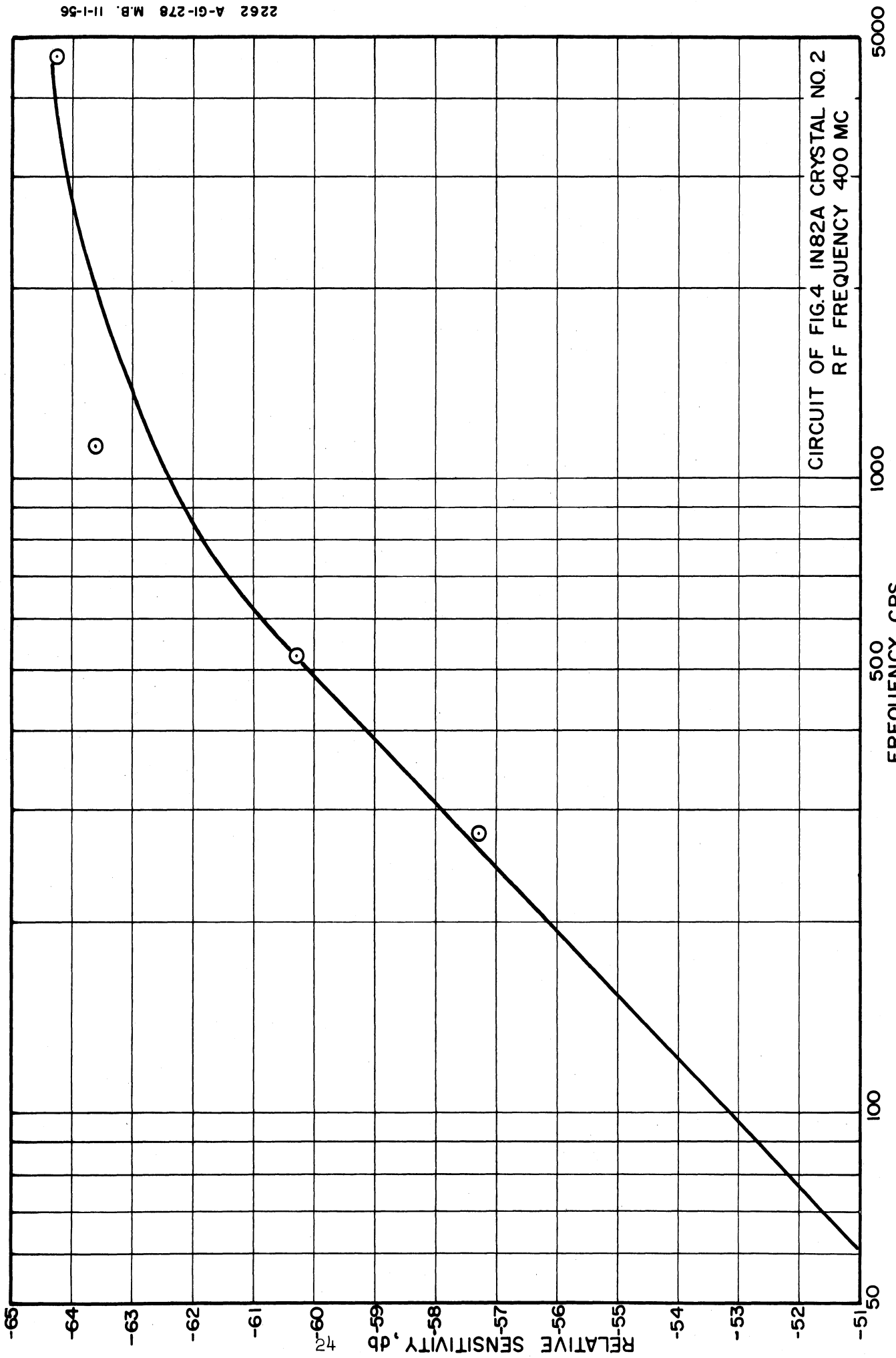
CIRCUIT OF FIG.4 IN82A CRYSTAL NO. 2
R F FREQUENCY 400 MC

FREQUENCY, CPS

RELATIVE SENSITIVITY, db

24

FIG. 14. VARIATION OF CRYSTAL VIDEO SENSITIVITY WITH INPUT MODULATION FREQUENCY

the RF signal to be detected, and the HP 200-AB audio oscillator supplies the

input modulation. The chopper signal is supplied by the external generator.

The output from the Brett circuit is fed to the circuit shown to the right of

line "xx" in Fig. 9.
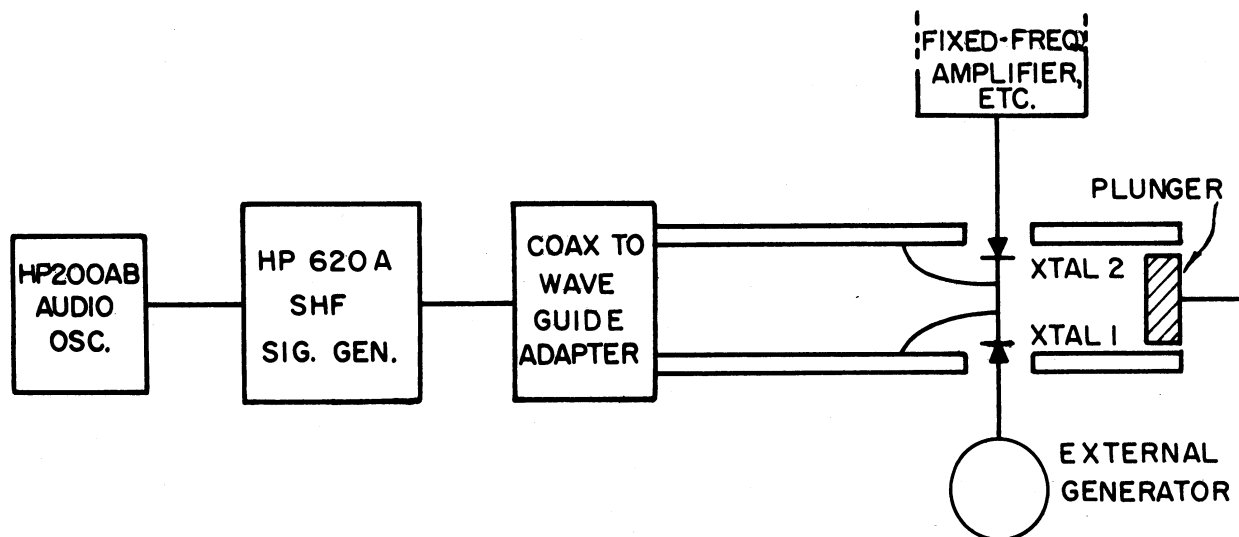
FIG. 15. EXPERIMENTAL BRETT CIRCUIT

To convert the above setup to a crystal video system the chopper

crystal (crystal 1) is replaced by a solid piece of brass (which provides a

short circuit to the case of the Brett structure), and the external generator,

the fixed-frequency amplifier, and the linear detector are removed.

6.2 Procedure

The first step in obtaining a sensitivity measurement with the Brett

circuit is to tune the HP 620-A SHF signal generator to the RF frequency desired.

The second step is to tune the external generator to the chopper frequency

desired and adjust its output level to a prescribed voltage. The third step

is to adjust the HP 200-AB audio oscillator to the center frequency of the 8 cps

bandwidth filter. The fourth step is to adjust the tuning stubs and waveguide

plunger to give the maximum signal output as indicated by the HP 400-B VTVM. The final step is to adjust the attenuator on the HP 620-A generator until the meter criterion previously described has been satisfied.

Chopper frequencies investigated were 60 and 2 mc. The fixed-frequency amplifiers used were those previously described. A HP 608-A VHF signal generator was used for the external generator in the 60 mc case, while a GR 1001-A signal generator was used in the 2 mc case.

There was a danger that a significant component of an observed output signal (HP 400-B reading) was due to direct feed-through of energy from the external generator. Such an output, which must occur in the audio band, would result because of incidental modulation of the external generator signal. To determine whether such an extraneous signal were present, the RF generator was turned off. The external generator signal level was then varied, and the variation in output observed. An external generator signal level was chosen at which a very small increase in output occurred. It was found that an appreciable extraneous output did not occur with an external generator signal level of 100 mv. This level was used in obtaining the data for making a comparison with the video system results.

To determine whether the increase in the no-signal output was actually feed-through, and not due to an increase in the effective crystal noise temperature ratio (t), an oscilloscope was attached to the output of the fixed-frequency amplifier. The external generator drive was then varied, and the resulting variation in output was observed on the oscilloscope. By this procedure, it was determined that the increase in output was primarily due to feed-through of the external generator signal.

Relative sensitivities for external generator voltages greater than 100 mv were obtained using the HP 608-A generator. These sensitivities, which are for a particular crystal and RF frequency, are presented in Fig. 16. Since the sensitivity increases for larger external generator signals than that which just produced a very small increase in the no-signal audio band output, a low noise external generator could be expected to give results superior to those of Fig. 16. It was felt that a crystal controlled oscillator would have the best output spectrum that could be readily obtained, and hence greater external generator drives might be employed before the no-signal audio band output increased appreciably. A 2 mc crystal-controlled oscillator was built, and the results obtained using it are presented in Fig.17.[1] It was found in this case that an appreciable extraneous output did not occur with an external generator signal level of 250 mv.

The corresponding crystal video sensitivities are obtained as outlined in the steps above except there is no chopper generator to adjust.

6.3 Results of Brett Circuit Measurements

Relative sensitivity for the actual Brett system and the corresponding crystal video system are presented in Fig. 18.[2] The Brett sensitivities were obtained with chopper voltages of 100 mv as previously explained. The variations of sensitivity with external generator voltages are presented in Figs. 16 and 17 as already described.

As indicated by these results, the sensitivities of Fig. 18 could be increased by about 4 db before being limited by feed-through by employing a crystal controlled oscillator.

---

1. The oscillator circuit is presented in Fig. 21.
2. The external generator for the data of Fig. 18 was the HP 608A.

Chopper Voltage (millivolts)	0 bias Sensitivity (dbm)	Opt. bias Sensitivity (dbm)
100	-65.0	-67.9 (.08 v.)
150	-68.0	-70.9 (.08 v.)
200	-68.5	-71.4 (.08 v.)
250	-69.0	-71.4 (.08 v.)
400	-69.0	-71.4 (.08 v.)

Figure 16

Sensitivities Obtained With Actual Brett Input Circuit for Various Chopper Voltages Using HP 608 as Ext. Generator (1N369A crystals used as chopper and detector, 60 mc chopper frequency 8.5 Kmc RF frequency.)

Chopper Voltage (millivolts)	0 bias Sensitivity (dbm)	Opt. bias Sensitivity (dbm)
100	-65.9	-68.6 (.05 v.)
250	-68.9	-71.6 (.05 v.)
500	-73.4	-75.6 (.05 v.)
1000	-73.4	-75.6 (.05 v.)
1400	-73.4	-75.6 (.05 v.)

Figure 17

Sensitivities Obtained With Actual Brett Input Circuit for Various Chopper Voltages Using Specially Built Crystal-Controlled Oscillator as Ext. Generator (1N369A crystals used as chopper and detector, 2 mc chopper frequency 8.5 Kmc RF frequency.)

Freq. (kmc)	Crystal Video Sensitivity (dbm)	60 mc Chopper Frequency Sensitivity (dbm)		2 mc Chopper Frequency Sensitivity (dbm)	
		0 bias	Opt. bias	0 bias	Opt. bias
8.5	-75.0	-65.0	-67.9 (.08 v.)	-66.4	-67.1 (.08 v.)
9.25	-74.5	-64.5	-66.4 (.08 v.)	-64.4	-66.1 (.08 v.)
10.0	-73.0	-61.0	-62.9/(.08 v.)	-61.9	-63.1 (.08 v.)
10.4	-71.5	-54.0	-57.9 (.08 v.)	-56.9	-58.6 (.08 v.)

Figure 18

Sensitivities Obtained With Actual Brett Input Circuit (1N369A crystals used as chopper and detector, chopper voltage 100 mv.)
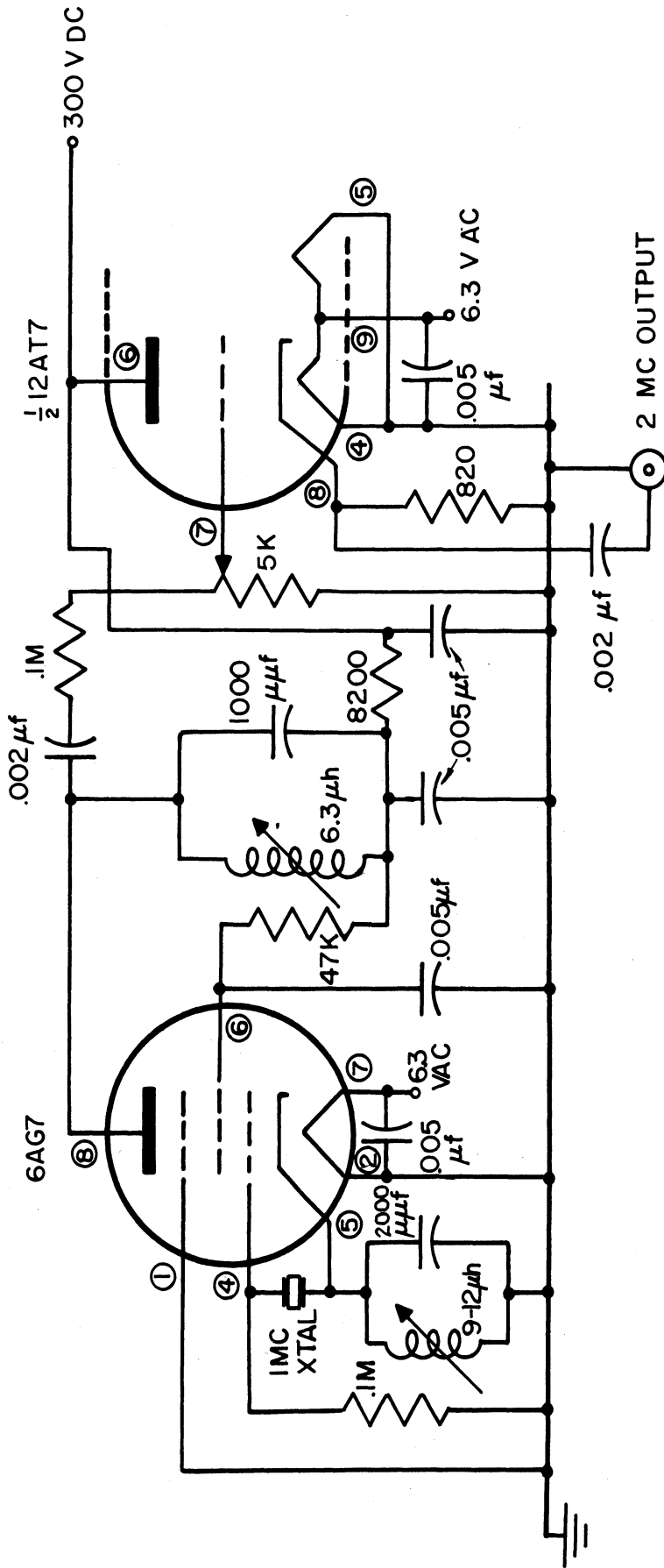
FIG. 19. CIRCUIT DIAGRAM OF 2 MC CRYSTAL-CONTROLLED OSCILLATOR

7. CONCLUSIONS

The results of the experimental investigation and the accompanying analysis indicate that a crystal video system has 0 to 6 db greater sensitivity than the Brett system for pulse repetition frequencies above 1000 pps. The Brett system appears to offer superior sensitivity for signals with a large duty factor (say 50%) at pulse rates less than approximately 100 pps.

The Brett system incorporates a conventional IF strip in place of the video amplifier of a crystal video system. Particular advantages which accrue relate to size and microphonics. In a mobile or portable broadband detection system, these advantages may be substantial.

APPENDIX

In this section, some general remarks concerning the principle of operation of the ESL circuits is presented. It seems desirable to preface this discussion with a brief mathematical statement of detection, mixing, and the apparent manner of operation of the Brett circuit.

Detection, as in a crystal video circuit, is achieved by impressing a signal

$$l = a(t) \cos \omega_0 t \qquad (A.1)$$

on a non-linear circuit. It is assumed that the transfer characteristic of the circuit can be expressed in the form

$$i_{out} = \alpha \, l_{in} + \beta l_{in}^2 + \dots \qquad (A.2)$$

For the case of low level detection the important output is due to the square law term

$$i_{out} = \beta \, a^2(t) \cos^2 \omega_0 t = \frac{\beta a^2(t)}{2} (1 + \cos 2 \, \omega_0 t) \qquad (A.3)$$

from which the useful output $\frac{\beta a^2(t)}{2}$ is selected by filtering. The output signal current is thus proportional to input power.

In the superheterodyne circuit, a local oscillator signal of frequency f_2 is utilized. For a diode mixer, then, a signal

$$l = a(t) \cos \omega_0 t + A \cos \omega_2 t \qquad (A.4)$$

is impressed on a circuit with a transfer characteristic such as in Eq A.2. The first few terms resulting from the substitution of Eq A.4 in Eq A.2, after utilizing some well known trigonometry identities, are:

$$i_{out} = \overbrace{\alpha a(t) \cos \omega_0 t + \alpha A \cos \omega_2 t}^{\text{linear terms}} + \overbrace{\frac{\beta a^2(t)}{2} (1 + \cos 2\omega_0 t) + \frac{\beta A^2}{2} (1 + \cos 2\omega_2 t)}^{\text{square law terms}}$$

$$\underbrace{+ \beta A a(t) \cos (\omega_0 - \omega_2)t + \beta A a(t) \cos (\omega_0 + \omega_2)t + \dots}_{\text{square law terms}} \qquad (A.5)$$

Ordinarily one of the latter two terms indicated would be filtered out as the useful output. Here the output signal current is proportional to the input signal voltage.

Consider the operation of the circuit of Fig. 2. After modulation and filtering, a signal

$$\ell = \frac{a(t)}{2} \left[1 + m\, g(t) \right] \cos \omega_0 t \tag{A.6}$$

is impressed on the demodulator, which has a transfer characteristic such as in Eq A.2. The function $g(t)$ depends on the modulation wave form chosen[1]. Substituting again in Eq A.2, the initial terms are

$$i_{out} = \frac{\alpha a(t)}{2} \left[1 + mg(t) \right] \cos \omega_0 t + \frac{\beta a^2(t)}{4} \left[1 + 2\, mg(t) + m^2 g^2(t) \right] \tfrac{1}{2}(1 + \cos 2\omega_0 t) \tag{A.7}$$

Let us suppose that the "periodic in time" function $g(t)$ can be expressed as a Fourier Series, and that a particular component of interest has amplitude g_n and frequency f_n. Writing only the outputs from the first two terms above which are due to the modulation component of frequency f_n,

$$
\begin{aligned}
i_{out} = {} & \frac{\alpha a(t)}{2} \left[1 + m\, g_n \cos (\omega_n t + \phi_n) \right] \cos \omega_0 t \\
& + \frac{\beta a^2(t)}{4} \tfrac{1}{2} \left[1 + 2\, mg_n \cos (\omega_n t + \phi_n) \right. \\
& + \frac{m^2 g_n^2}{2} \left\{ 1 + \cos 2(\omega_n t + \phi_n) \right\} \left. \right] (1 + \cos 2\omega_0 t) + \ldots\ldots \tag{A.8}
\end{aligned}
$$

Consider the term

$$\frac{m\beta a^2(t)}{2}\ g_n \cos (\omega_n t + \phi_n)\ .$$

This output current component, which is centered around the frequency ω_n, contains the input modulation information, and is zero when the modulator is turned off. It is proportional to the curvature of the crystal characteristic

---

1. The reduction in peak amplitude due to modulator losses is not considered here. The function $g(t)$ is assumed to vary periodically between +1 and -1. The degree of modulation achieved at the modulator is indicated by the modulation index m.

and to input power, just as for straight detection. The other signal components displayed above are video or RF except for a term centered around $2\omega_n$ which is also potentially useful but is smaller than the ω_n terms. If higher order terms of the power series of the transfer characteristic are considered, outputs centered at higher harmonics of ω_n are among those present, but generally can be expected to be smaller than the output at ω_n.

It is perhaps worth pointing out that for sinusoidal modulation, $g = \cos(\omega t + \theta)$. The Fourier Series is in this case very simple, containing just one component of unit amplitude and frequency. f. The largest g_n which can occur is readily shown to be realized for the fundamental component of a square wave, when $g_1 = 4/\pi$. In a practical circuit a loss accrues from the fact that m is less than unity.

It is interesting to consider whether the analysis of Fig. 2 just presented is a valid description of the operation of the circuit of Fig. 1. Referring to Fig. 1, the leads designated as filters are intended to be essentially short circuits to the external generator signal, and to have nominal RF impedances. Then the external generator voltage causes a current to flow which is largely confined to the path indicated in Fig. 1. This current can reasonably be expected to effect a variation of the RF impedance of crystal 1, and thus a variation of RF absorption of crystal 1. In fact, this clearly would be the only important effect of the external generator signal if the external generator current were confined to the path mentioned above.

Now, one might expect that as a result of the varying absorption of crystal 1, the RF signal absorbed by the circuit of crystal 2 would also vary (with, of course, the same periodicity). This is tantamount to modulation of the RF signal by the circuit of crystal 1.

REFERENCES

1. R. A. Smith, "The Relative Advantages of Coherent and Incoherent Detectors: A Study of Their Noise Spectra Under Various Conditions," Proc. IEE, 89, Part 3, Sept. 1951.

2. Torrey and Whitmer, "Crystal Rectifiers", MIT Rad. Lab. Series, Vol. 15, McGraw-Hill, 1948.

3. Van Voorhis, et. al., "Crystal Detectors and the Crystal-Video Receiver," Report 638, MIT Radiation Laboratory.

4. H. Wallman, C. P. Gadsten, A. B. Macnee, "A Low Noise Amplifier," Proc. IRE, June 1948.

5. J. L. Lawson, G. E. Uhlenbeck, "Threshold Signals," Rad. Lab. Series, Vol. 24, McGraw-Hill, 1950.

1 Copy	Document Room Stanford Electronic Laboratories Stanford University Stanford, California
1 Copy	Commanding General Army Electronic Proving Ground Fort Huachuca, Arizona Attn: Director, Electronic Warfare Department
1 Copy	Chief, Research and Development Division Office of the Chief Signal Officer Department of the Army Washington 25, D. C. Attn: SIGEB
1 Copy	Chief, Plans and Operations Division Office of the Chief Signal Officer Washington 25, D. C. Attn: SIGEW
1 Copy	Commanding Officer Signal Corps Electronics Research Unit 9560 TSU Mountain View, California
40 Copies	Transportation Officer, SCEL Evans Signal Laboratory Building No. 42, Belmar, New Jersey FOR- SCEL Accountable Officer Inspect at Destination File No. 22824-PH-54-91 (1701)
1 Copy	J. A. Boyd Engineering Research Institute University of Michigan Ann Arbor, Michigan
1 Copy	Document Room Willow Run Laboratories University of Michigan Willow Run, Michigan
12 Copies	Electronic Defense Group Project File University of Michigan Ann Arbor, Michigan
1 Copy	Engineering Research Institute Project File University of Michigan Ann Arbor, Michigan